Available online at www.sciencedirect.com
SCIENCE DIRECT®
Biochemical Pharmacology 65 (2003) 1817–1826
Biochemical Pharmacology
www.elsevier.com/locate/biochempharm

An amperometric biosensor with human CYP3A4 as a novel drug screening tool☆

Shiba Joseph[a], James F. Rusling[b], Yuri M. Lvov[c], Thomas Friedberg[d], Uwe Fuhr[a,*]

[a]*Institute for Pharmacology, Clinical Pharmacology, University of Köln, Köln, Germany*
[b]*Department of Chemistry, University of Connecticut, Connecticut, New Haven, CT, USA*
[c]*Institute for Micromanufacturing, Louisiana Tech University, Ruston, LA 71272, USA*
[d]*Biomedical Research Center, University of Dundee, Dundee, UK*

Received 30 September 2002; accepted 18 February 2003

Abstract

We developed a biosensor based on the redox properties of human CYP3A4 to directly monitor electron transfer to the heme protein. Enzyme films were assembled on gold electrodes by alternate adsorption of a CYP3A4 layer on top of a polycation layer. Direct, reversible electron transfer between the electrode and CYP3A4 was observed with voltammetry under anaerobic conditions. In the presence of oxygen, the oxidation peak of the hemoprotein disappeared, and the reduction peak increased 2- to 3-fold. Addition of CYP3A4 substrates (verapamil, midazolam, quinidine, and progesterone) to the oxygenated solution caused a concentration-dependent increase in the reduction current in cyclic voltammetric and amperometric experiments. Product analyses after electrolysis with the enzyme film showed catalytic activity of the biosensor depending on substrate concentration, its inhibition by ketoconazole, and a minor contribution of H_2O_2 to the catalytic cycle. These results suggest that electron exchange between the electrode and the immobilized CYP3A4 occurred, and that metabolic activity of the enzyme was maintained. Thus, important requirements for the application of human CYP biosensors in order to identify drugs or drug candidates as substrates or inhibitors to the attached enzyme are fulfilled.

Keywords: Biosensor; CYP3A4; Amperometry; Cyclic voltammetry; Cytochrome P450; Midazolam; Verapamil

1. Introduction

The members of the P450 enzyme superfamily often mediate rate-limiting steps in the metabolism of xenobiotics, including many drugs and environmentally relevant small molecules. The P450s may inactivate drugs or toxic chemicals or activate them to effective, mutagenic, and/or carcinogenic forms [1,2]. P450s also metabolize endogenous compounds, such as steroids, fatty acids, and prostaglandins [3,4]. Thus, characterization of these enzymes is a key issue in pharmacokinetics and in toxicokinetics as well as in regulation of some endogenous metabolic pathways.

Activity of P450s is currently determined from the rates of formation of metabolites. Measurement of metabolite concentration requires development and maintenance of methods for each metabolic pathway examined. Another possible approach that is applicable, irrespective of the substrate and the individual P450, is to measure the consumption of co-factors of the reaction, i.e. of oxygen and NADPH. However, these co-factors need to be present in excess in order to avoid any influence on enzyme activity, and it is not always possible to reliably determine small changes in concentrations of these co-factors.

As a direct approach based on the redox properties of P450s, we have developed an amperometric biosensor which allows one to follow its catalytic cycle by monitoring electron transfer to the enzyme. A biosensor could replace existing techniques of measuring enzyme activity. No natural redox partner is required because an electrode

☆This work was supported by the Köln Fortune Program and by Grant No. ES03154 from the National Institute of Environmental Health Science (NIEHS), NIH, USA.
* Corresponding author. Tel.: +49-221-478-5230; fax: +49-221-478-7011.
E-mail address: uwe.fuhr@medizin.uni-koeln.de (U. Fuhr).

Abbreviations: CV, cyclic voltammetry; CYP, cytochrome P450; D-617, *N*-methyl-4-(3,4-dimethoxyphenyl)-4-cyano-5-methylhexylamine; MPS, 3-mercapto-1-propenesulfonic acid; MDZ, midazolam; PDDA, poly-(dimethyldiallylammonium chloride); QCM, Quartz Crystal Microbalance; SWV, square wave voltammetry; SCE, saturated calomel electrode.

0006-2952/03/$ – see front matter © 2003 Elsevier Science Inc. All rights reserved.
doi:10.1016/S0006-2952(03)00186-2

directly supplies the electrons required to drive P450-mediated catalysis. The direct monitoring of electron transfer may also be useful to further elucidate the complex chemical processes taking place during P450-mediated reactions.

Achieving an electrical communication between an electrode and an enzyme is the pivotal step in the development of amperometric biosensors [5]. However, usually the protein matrix may insulate the redox site from direct electron transfer [6]. Additionally, adsorptive denaturation of the enzyme and macromolecular impurities on the electrode may impede electron transfer. These problems may be overcome by a specific binding of the enzymes to the surface of an electrode [7,8]. While various enzyme immobilization techniques have been reported to establish electrical communication in enzyme-electrode assemblies, methods must often be designed empirically for the specific enzyme under study [6]. With respect to P450 biosensors [9,10], there are currently only a few reports available. Most studies used the soluble CYP101. Direct electron transfer to CYP101 has been shown for a variety of electrode interfaces, including pyrrolytic graphite [11,12], gold [13], glassy carbon [14], platinum [10], and indium tin oxide [15]. CYP101 embedded in polyion films on electrodes was used to catalyze the oxidation of styrenes to styrene oxides [13,16]. In addition, catalytic activity had been shown by the hydroxylation of camphor. For biosensors with membrane-bound CYPs, non-human enzymes bound to a mediator such as fusion proteins of CYPs with NADPH-cytochrome P450 (CYP) oxidoreductase [17] or CYPs covalently bound to small molecules such as riboflavin [18] have been used. Again, electron transfer and catalytic activity could be shown.

The objective of the present work was to develop such a biosensor for a membrane-bound human P450 not modified by mediators bound to the enzyme. Its intended application is to identify drugs or drug candidates as substrates or inhibitors to the enzyme bound to the biosensor. We focused on CYP3A4 because it is currently believed to be the most important of the P450s in drug metabolism.

2. Materials and methods

Purified CYP3A4 (MW 51500 Da) was prepared as described [19]. Chemicals used for film assembly were poly-(dimethyldiallylammonium chloride) (PDDA) (Aldrich) and 3-mercapto-1-propenesulfonic acid (MPS) (Fluka). The substrates of CYP3A4 (verapamil, quinidine, and progesterone) and superoxide dismutase were purchased from Aldrich. Midazolam (MDZ) was obtained from Hoffmann-La Roche AG. Catalase and ketoconazole were purchased from ICN Biomedicals GmbH. Quantofix Peroxide sticks for the detection of H_2O_2 were from Machenerey-Nagel.

2.1. Instrumentation

A Quartz Crystal Microbalance (QCM; USI System) was used to monitor the formation of enzyme films on the electrode. The quartz resonators (AT-cut; USI System) used were covered by gold electrodes on both faces and their resonance frequency was 9 MHz. A BAS 100 B/W electrochemical analyzer was used for cyclic voltammetry (CV) and square wave voltammetry (SWV). Electrolysis experiments and amperometry were done with a potentiostat model PGSTAT 10 (Metrohm). The three-electrode electrochemical cell had a saturated calomel electrode (SCE) or a Ag/AgCl electrode as reference electrode and a palladium wire counter electrode. Working electrodes for CV, SWV, and amperometry were ordinary gold discs (3 mm diameter; Metrohm). A 2.2 cm × 1.1 cm gold foil (Alpha Aesar) was used as working electrode for the electrolysis.

2.2. Methods

2.2.1. Preparation of enzyme electrodes

Single layer and multilayer films were assembled on gold electrodes of the QCM resonator and on gold discs as follows [13]: First, electrode surfaces were washed with a cleaning solution (ethanol:water:KOH; 60:39:1) and polished with aqueous slurries of alumna. A negatively charged gold surface was then prepared by coating with MPS (1 mM). Films were grown by alternate adsorption from an aqueous solution of PDDA (2 mg/mL) or from a 19.4 μM suspension of human CYP3A4 in 50 mM phosphate buffer containing 100 mM KCl and 6.2% glycerol. To this end, electrodes were first immersed for 20 min in the PDDA solution and then for 20 min in the enzyme suspension, with intermediate washing with ultrapure water. Films were dried under a stream of nitrogen at room temperature after each immersion in the sensor reagents. Up to 10 molecular layers of enzyme were coated over the gold resonator for monitoring of film growth. For the electrochemical experiments, single layer and multilayer enzyme film-coated gold electrodes were prepared.

2.2.2. Monitoring of enzyme film formation by QCM

To monitor film growth, the change in the resonance frequency of the MPS-modified gold electrode was registered after each adsorption step. The mass increase that occurred for each adsorption step was estimated from the frequency change Δf using the Sauerbrey equation (Eq. (1)) [20].

$$\Delta f = -\frac{f_0^2}{N\rho_q}\Delta\left(\frac{M}{A}\right) \quad (1)$$

where Δf, change in frequency (Hz); f_0, fundamental resonance frequency of the crystal (Hz); N, frequency constant (1670 kHz m^2); ρ_q, density of quartz (g/cm^3),

$\Delta(M/A)$, change in mass M (g) per area A on which the deposit of the film occurs, corresponding to an apparent area of the quartz crystal placed between QCM electrodes (cm^2).

As the fundamental resonance frequency of the QCM is known, the measured frequency shifts for dry films can be directly transformed into a mass increase, resulting in the simplified Sauerbrey equation (Eq. (2)).

$$\Delta f = -1.832 \times 10^8 \, \Delta\left(\frac{M}{A}\right) \quad (2)$$

For explanation of symbols, see legend to Eq. (1).

From the area of the deposition (0.16 ± 0.01 cm^2), the thickness of the films on both sides of the electrode was then derived as described in Eq. (3) [21] assuming an approximate density of 1.3 ± 0.1 g/cm^3 for enzyme and 1.2 ± 0.1 g/cm^3 for polyion film [22].

$$d\,(\text{Å}) \approx -0.16\,\Delta f\,(\text{Hz}) \quad (3)$$

where d is the thickness of the film.The molecular diameter of CYP3A4 was assumed to be about 35–40 Å.[1]

2.2.3. Electrochemistry

CV, SWV, amperometry, and electrolysis were applied. For CV an initial potential is changed in a linear manner up to a pre-defined limit and then reversed to the initial value. During this process, the Faradaic current response is measured. The resulting cyclic voltammogram and its parameters, mainly the two peak currents and two peak potentials (Fig. 1), provide the basis for analyzing the redox reaction. In SWV the potential is applied as a ramped square wave and the current is measured between just before and near the end of each pulse. CV and SWV experiments were carried out in a 10 mL electrochemical cell containing 0.05 M phosphate buffer (pH 7.4) with 100 mM KCl in which were placed a palladium counter electrode and a saturated calomel reference electrode (SCE). Single and multiple layer enzyme-loaded gold discs were used as working electrodes to examine the number of electroactive layers; because only the first layer was found to be electroactive (see below), further experiments were conducted with single layer electrodes. Temperature was controlled at 25°. The working electrode was cycled between initial and switch potentials of 300 and −600 mV, respectively. Prior to CV and SWV, solutions were degassed by bubbling with purified nitrogen (cyclic voltammetric experiments) or argon (amperometric experiments) for 30 min and a layer of the respective inert gas was maintained on the top of the cell. When needed, pure oxygen was added to the solutions. Voltammograms were taken in the absence and in the presence of oxygen and/or substrates to observe the enzyme–oxygen–substrate interaction.

[1] Personal communication with Dr. D. Kirill, European Bioinformatics Institute, Cambridge, UK.

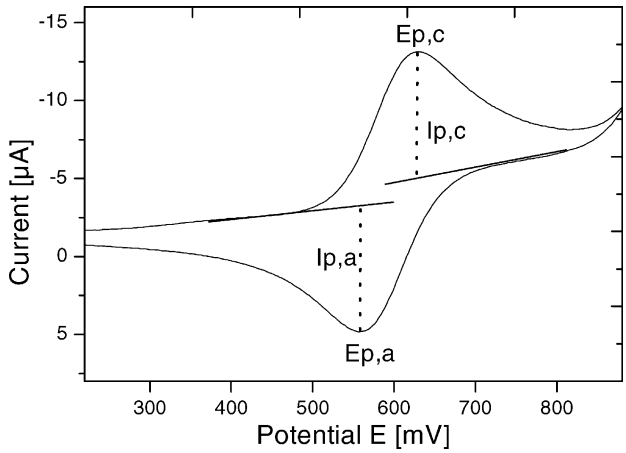

Fig. 1. A typical cyclic voltammogramm of an electroactive redox couple. $I_{p,a}$: anodic peak current; $I_{p,c}$: cathodic peak current; $E_{p,a}$: anodic peak potential; $E_{p,c}$: cathodic peak potential.

The formal potential of CYP3A4 was estimated from cyclic voltammetric data as a midpoint potential (Eq. (4)).

$$E_m = \frac{1}{2}(E_{p,a} + E_{p,c}) \quad (4)$$

where $E_{p,a}$ and $E_{p,c}$ are anodic peak potential and cathodic peak potential, respectively.

Integration of the reduction peak observed for electron transfer by CV using anaerobic conditions gave the amount of charge (Q) transferred on reduction of CYP3A4. The surface concentration of electroactive enzyme on the electrode was then estimated by assuming the one electron transfer by using Faraday's Law:

$$Q = mF \quad (5)$$

where Q, charge (C); m, mass of electroactive species (mol); F, Faraday's constant (96485 C/mol).

For amperometric measurement, a 10 mL electrochemical cell thermostated at 25° was used in a three-electrode configuration, consisting of a palladium counter electrode and a Ag/AgCl reference electrode. The working electrode (single layer CYP3A4 adsorbed gold disc) was polarized at −450 mV vs. Ag/AgCl. Prior to injecting 10 mL of oxygen gas into the 50 mM phosphate solution containing 100 mM KCl, the cell was degassed as described above. The background current was allowed to decay to a steady state, then aliquots of 400 µL of 10 mM verapamil (for resulting concentrations of verapamil in reaction cell see Fig. 5) were added at regular intervals. The solution was stirred constantly throughout the whole experiment and steady-state amperograms were recorded. Amperometric experiments were also done with other CYP3A4 substrates (MDZ, progesterone, and quinidine).

Electrolyses were carried out for the catalytic dealkylation of verapamil and hydroxylation of MDZ at −500 mV vs. Ag/AgCl in a 5 mL electrochemical cell containing 50 mM phosphate solution with 500 µM verapamil or 50 µM MDZ, respectively. A 2.2 cm × 1.1 cm gold foil

(effective area) loaded with a single layer of CYP3A4 on both sides was used as the working electrode. Since oxygen is essential to activate CYP3A4 for the catalytic reaction, electrolyses were carried out in aerobic conditions. During the electrolysis, samples were taken at pre-defined points of time up to 2 hr and analyzed by LC/MS for metabolite formation. Samples were also taken after 60 min and analyzed with Quantofix Peroxide sticks to detect hydrogen peroxide. Further, electrolyses of verapamil and MDZ were carried out in the presence of ketoconazole, a CYP3A4 inhibitor (500 μM), and of catalase (60 U/mL) or superoxide dismutase (700 ng/mL) to assess the role of reactive oxygen in metabolite formation. Incubations of 500 μM verapamil for 40 min and of 50 μM MDZ for 30 min were also carried out with 100 μM H_2O_2 in a 4 mL glass vessel under the same experimental conditions used for electrolysis in the presence and in the absence of enzyme-coated electrode without using an electromotive force. Products of incubations were analyzed by LC/MS.

The LC/MS analyses of verapamil metabolites [23] and MDZ metabolites (procedure not published) were carried out in Dr. Margarete Fischer, Bosch, Institut für klinische Pharmakologie, Stuttgart, Germany, and in Bayer AG, Abt. Metabolismus und Isotopenchemie, Wuppertal, Germany, respectively.

3. Results

3.1. Assembly of the CYP3A4/polycation film

Assembly of films containing alternate layers of CYP3A4 and positively charged PDDA was characterized by QCM. The QCM monitoring showed a linear change of the resonance frequency with cycles of adsorption on MPS-modified gold electrodes. This indicates a linear increase of film mass with increasing number of cycles.

For every layer of CYP3A4, QCM frequency (f) decreased by (mean ± SD) 250 ± 11.4 Hz. Each PDDA adsorption step caused a frequency decrease of about 50 ± 2.2 Hz. According to Eqs (1)–(3) (see above), a mean mass increase of 225 and 45 ng was found for one layer of CYP3A4 and PDDA film, respectively. This means that about 27 pmol of CYP3A4 was present per cm^2 on the surface of the biosensor. These masses correspond to a 40 ± 4 Å thickness for each CYP3A4 layer and 8 ± 0.8 Å thickness for the polycation layer.

3.2. Electroactivity of the CYP3A4/polycation film

Electrochemical characterization of the enzyme-bound film was done by CV and by SWV. Cyclic voltammograms of a solution of 7.3 nM CYP3A4 in an anaerobic buffer at a bare electrode gave no redox peaks (Fig. 2). The CYP3A4/PDDA film-loaded gold electrode gave well-defined redox peaks by CV (Fig. 2), which could be observed only after an equilibration time of 50–60 min. Gold electrodes loaded with multiple layers of CYP3A4 gave similar CVs with nearly the same peak currents as those for a single enzyme layer. Redox potential of the CY3A4 (Fe^{III})/(Fe^{II}) couple in the film, estimated as the midpoint (E_m) between anodic and cathodic peak potentials, was 98 ± 5 mV vs. normal hydrogen electrode (NHE). The separation between the reduction and the oxidation peaks, which had nearly the same heights, was about 98 mV. The peak current showed a linear dependence on the scan rate from 100 to 2000 mV/s. Integration of the reduction peak showed that about 1.9 μC/cm^2 was transferred on reduction of CYP3A4. This means that about 19.6 pmol of electroactive CYP3A4 was present per cm^2 on the surface of the biosensor (Eq. (5)). This was about 70% of adsorbed enzyme determined using the QCM.

Reversible SWVs were obtained for the CYP3A4 biosensor. An E_m value of about 91 mV vs. NHE was estimated from the forward and reverse redox peaks.

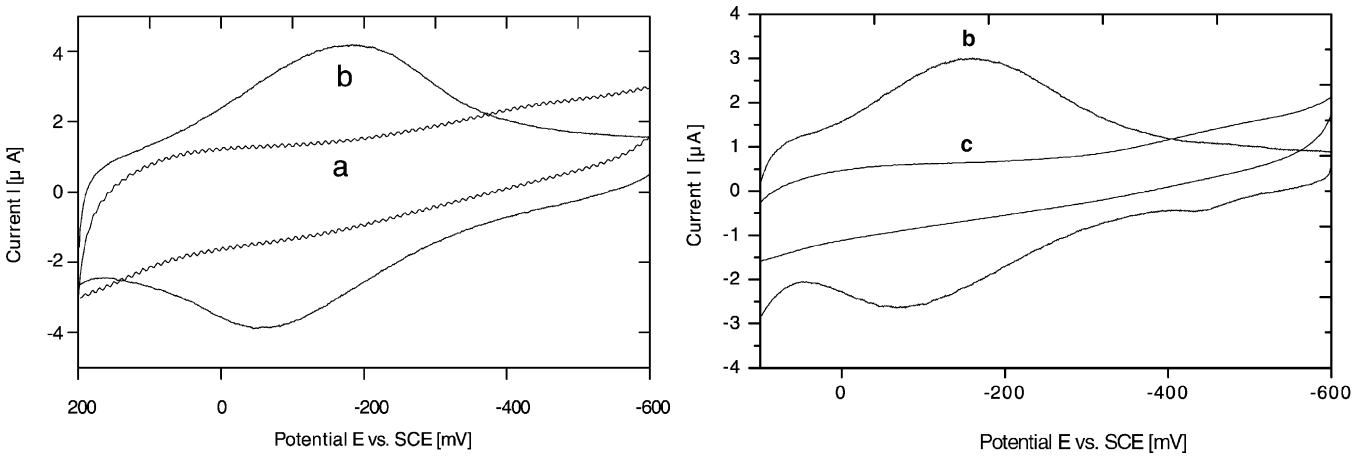

Fig. 2. Cyclic voltammograms showing the enhanced electron transfer between gold electrode and immobilized enzyme compared to a dilute enzyme suspension (7.3 nM). Experiments were carried out at 100 mV/s in pH 7.4 phosphate buffer containing 100 mM KCl. (a) Bare gold electrode in buffer containing 7.3 nM CYP3A4. (b) Au/MPS/PDDA/CYP3A4 film in buffer containing no enzyme. (c) Au/MPS/PDDA electrode without CYP3A4 in buffer containing no enzyme.

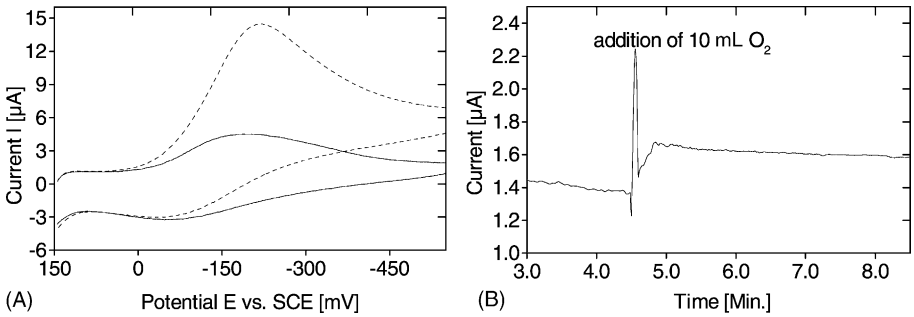

Fig. 3. Effect of oxygen on the behavior of the CYP3A4 biosensor. (A) Cyclic voltammetry of Au/MPS/PDDA/CYP3A4 electrode in 0.05 M phosphate buffer/0.1 M KCl in the absence (solid line) and in the presence of oxygen (dashed line). (B) Amperometric response of Au/MPS/PDDA/CYP3A4 electrode upon the injection of 10 mL oxygen into the 10 mL buffer solution. The gold electrode was polarized at −450 mV for the amperometric experiments.

3.3. Catalytic activity of the CYP3A4 biosensor

CV (Figs. 3A and 4) and amperometry (Figs. 3B and 5) were used to study the catalytic behavior of the of MPS/PDDA/CYP3A4 films. In the presence of oxygen, greatly increased reduction peaks (at 200 mV/s) and almost no oxidation peaks were observed. At scan rates higher than 500 mV/s, the oxidation peak was again visible. Direct reduction of oxygen occurred at −500 mV vs. SCE on gold electrodes loaded only with PDDA.

The effect of substrates on the electroactivity of the CYP3A4 biosensor was studied by CV, SWV, and amperometry. Fig. 4 shows the voltammetric responses of the CYP3A4-loaded gold electrode in the presence and in the absence of verapamil. Voltammograms showed a markedly increase in the reduction current upon the addition of verapamil to the oxygen-containing solution. In the absence of oxygen, the addition of substrates to the buffer solution gave no noticeable change in reduction current and in reduction potential.

The amperometric measurements showed a measurable change in current upon the subsequent addition of verapamil up to a final concentration of 2.85 mM. Fig. 5 shows the steady-state responses of the biosensor and steady-state calibration curve for verapamil. The response time to reach 95% of the steady state was approximately 15–25 s. The enzyme electrode exhibited a linearity of calibration up to

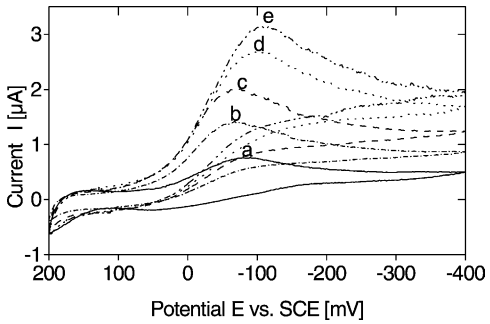

Fig. 4. Voltammetric response of the CYP3A4 biosensor upon the addition of verapamil. Cyclic voltammograms at 10 mV/s for the Au/MPS/PDDA/CYP3A4 electrode were recorded (a) in the absence of oxygen and substrate, or following injection of 10 mL of oxygen gas and (b) 0 mM verapamil, (c) 0.87 mM verapamil, (d) 2.48 mM verapamil, or (e) 3.21 mM verapamil.

2.85 mM. The slope of the linear range was 1.46×10^3 µA/M with a correlation coefficient of 0.998. The typical plateau in calibration curves derived from enzymatic reactions could not be observed. The poor solubility of verapamil in buffer (<4 mM in phosphate buffer, pH 7.4) at higher concentrations did not allow us to measure the real response to this substrate at a concentration above 2.85 mM. The amperometric studies with other substrates (MDZ, progesterone, and quinidine) also showed a concentration-dependent change in reduction current upon

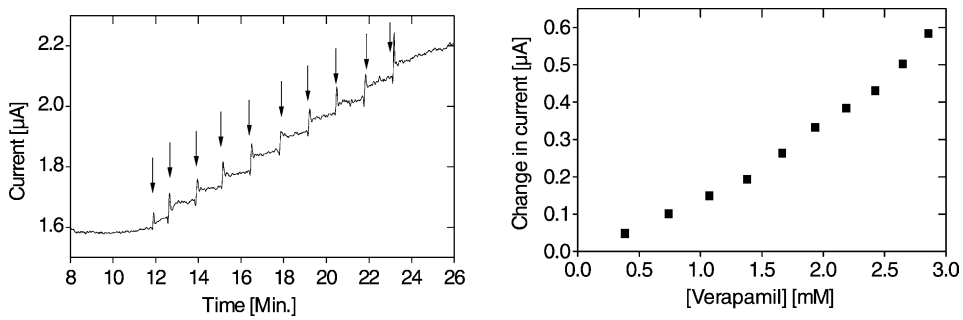

Fig. 5. Steady-state amperometric responses of the CYP3A4 biosensor upon addition of verapamil, a CYP3A4 substrate. Four hundred microliters aliquots of 10 mM verapamil (see calibration curve for concentration of verapamil in the reaction cell) were added successively (↓) into the electrochemical cell containing 10 mL of 50 mM phosphate buffer/100 mM KCl. The amperometric response of the Au/MPS/PDDA/CYP3A4 electrode at −450 mV (left) gave a calibration curve for verapamil (right).

Table 1
Verapamil dealkylation under different experimental conditions

System[a]	Verapamil metabolites[b]				Midazolam metabolites[c]			
	D-617		Norverapamil (μM)		1′-Hydroxymidazolam		4-Hydroxymidazolam	
	Concentration (μM)	Product formation rate[d]	Concentration (μM)	Product formation rate[d]	Concentration (nM)	Product formation rate[d]	Concentration (nM)	Product formation rate[d]
Electrolysis with Au/MPS/PDDA electrode	0.27	n.a.	0.21	n.a.	6.5	n.a.	8	n.a.
Electrolysis with Au/MPS/PDDA/CYP3A4 electrode	3.18	5.31	2.44	4.12	264	0.588	45	0.098
Electrolysis with Au/MPS/PDDA/CYP3A4 electrode/500 μM ketoconazole	0.65	1.08	0.48	0.82	48	0.100	12	0.027
Electrolysis with Au/MPS/PDDA/CYP3A4 electrode/catalase (60 U/mL)	1.61	2.68	1.6	2.68	195	0.433	35	0.077
Electrolysis with Au/MPS/PDDA/CYP3A4 electrode/superoxide dismutase (700 ng/mL)	3.51	5.82	2.48	4.12	334	0.742	37	0.082
Incubation, no voltage impressed (Au/MPS/PDDA/CYP3A4 electrode + 100 μM H_2O_2)	1.32	2.22	1.01	1.86	57	0.126	12	0.027
Incubation, no voltage impressed (no electrode, 100 μM H_2O_2)	0.12	n.a.	1.1	n.a.	<Detection limit	n.a.	<Detection limit	n.a.

Electrolyses of verapamil (500 μM) and midazolam (50 μM) were carried out at −500 mV vs. Ag/AgCl under aerobic conditions in phosphate buffer, pH 7.4. Additional incubations with H_2O_2 were carried out without using an electromotive force under the same experimental conditions used for electrolysis. Metabolite concentrations were determined by LC/MS. Detection limits for metabolites of verapamil and midazolam were 1 pmol and 150 fmol, respectively.

[a] Contains 500 μM verapamil or 50 μM midazolam, 50 mM phosphate buffer (pH 7.4), 100 mM KCl.

[b] Electrolysis and incubation time was 40 min.

[c] Electrolysis and incubation time was 30 min.

[d] Unit: nmol/min/nmol CYP3A4.

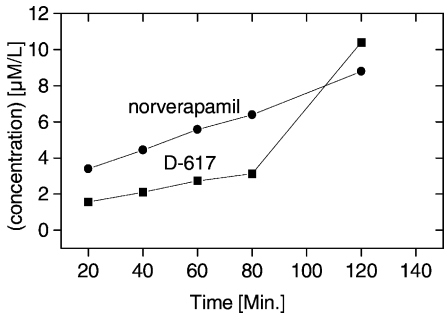

Fig. 6. Metabolites formation during electrolysis. Electrolyses of verapamil (500 µM) were carried out using Au/MPS/PDDA/CYP3A4 electrodes under aerobic conditions in phosphate buffer, pH 7.4. The working potential was −500 mV vs. Ag/AgCl. Metabolite concentrations were determined by LC/MS. The diagram shows time-dependent formation of verapamil metabolites.

their addition in to the reaction cell. As the reaction for these substrates followed Michaelis–Menten kinetics, apparent K_m values could be calculated from amperometric data for MDZ, progesterone, and quinidine and reached 547 ± 57 µM, 271 ± 71 µM, and 1082 ± 353 µM, respectively.

Electrolyses at −500 mV vs. Ag/AgCl in pH 7.4 buffer solutions containing 500 µM verapamil in the presence of oxygen using the CYP3A4 biosensor produced *N*-methyl-4-(3,4-dimethoxyphenyl)-4-cyano-5-methylhexylamine (D-617), the dealkylated metabolite and norverapamil, the demethylated metabolite, as major products. The amounts of products increased with electrolysis time (Fig. 6). Yield of D-617 was 13-fold larger compared to control electrolyses using the same electrode with no CYP3A4 loading. The average product formation rates we measured for D-617 and for norverapamil were 5.05 and 4.23 nmol/min/nmol CYP3A4, respectively (Table 1). Ketoconazole inhibited the product formation by about 80%. Presence of catalase in the reaction mixture led to a 50% reduction of product formation. Superoxide dismutase showed no obvious influence on metabolite formation (Table 1). The incubation of verapamil with H_2O_2 and CYP3A4-coated electrode without using an electromotive force yielded D-617 and norverapamil as products (Table 1), but the product formation rates were reduced to 30%. When enzyme was omitted from the incubation system, only norverapamil was detected. Clearly more H_2O_2 (2–3 mg/L) was detected after 1 hr electrolysis with a CYP3A4-coated electrode than in control electrolysis with an electrode not coated with CYP3A4 (<0.5 mg/L).

Electrolysis of 50 µM MDZ at −500 mV vs. Ag/AgCl under aerobic conditions using the CYP3A4 biosensor yielded 1′-hydroxymidazolam and 4-hydroxymidazolam as products. The product formation rate for 1′-hydroxylation and for 4-hydroxylation was 0.59 and 0.10 nmol/min/nmol CYP3A4, respectively. The concentration of metabolites increased almost in a linear relationship to time of electrolysis. The influence of catalase, H_2O_2, ketoconazole, and superoxide dismutase on the MDZ metabolism was comparable with that found for verapamil metabolism (Table 1).

4. Discussion

The present study demonstrates the feasibility of using a detergent-solubilized and purified membrane-bound P450 deposited as monolayers on electrodes as biosensors. The CYP3A4/polycation films constructed on MPS/gold electrodes by alternate layer-by-layer adsorption of protein were mechanically and electrochemically stable for 10–15 days, about the same period for which the enzyme is active. Alternate adsorption of layers of polycation and enzyme on electrode surfaces was confirmed by QCM. QCM frequency changes for polycation and enzyme adsorption steps correlate approximately with their respective molecular weights. Estimated enzyme layer thickness suggests monolayer formation. However, this conclusion is valid only if orientation, packing density, and hydration of the enzyme in the layer do not have a significant influence on enzyme layer thickness.

CV and SWV done with the enzyme-loaded gold electrode showed that reversible electrochemical conversion of the CYP3A4 (Fe^{III}) to CYP3A4 (Fe^{II}) was achieved in the PDDA/CYP3A4 film. The reduction peak on the forward scan suggests direct electron transfer from the electrode to the heme protein. The peak on the reverse scan indicates the re-oxidation of the reduced enzyme. Electron transfer between the electrode and the adsorbed enzyme at the concentrations used is much improved over that in solution, where it could not be observed by voltammetry (Fig. 2). Possible reasons for the improved Fe^{III}/Fe^{II} electrochemistry in the films include the relatively high concentration of enzyme close to the electrode and inhibition of adsorption and denaturation of proteins on electrodes by adsorbed ionic film components [5].

The midpoint potential for immobilized CYP3A4 obtained from voltammetry is not the same as that measured for P450s in solution by the potentiometric titration method. Compared to the measured midpoint potential of CYP101 of −250 mV [24], E_m is shifted by about 350 mV in the positive direction. This discrepancy may be caused by the possible differences in the heme environment of the P450 in solution and in immobilized state. The electrostatic interaction of enzyme–polyion in the film may significantly control the redox potential of the heme iron. [25]. For instance, compared to the solution value, the redox potential of myoglobin in polyion film is shifted by 133 mV in the negative direction [26], whereas the potential of CYP101 bound to a glassy carbon electrode modified with sodium montmorillonite was positively shifted by 164 mV compared to the potential of the enzyme in solution [14].

The appearance of voltammetric redox signals only after an equilibration time of an hour in buffer may be explained

by the need for full hydration of the film, and possible reorientation of the enzyme. Surface reorganization of polyions after an initial rapid adsorption to surfaces has been documented previously [26]. After equilibration, the linear dependence of the peak current on scan rate and the nearly equal oxidation and reduction peak heights indicate the so-called ''thin layer'' electrochemical behavior [27], in which all electroactive CYP3A4 in the ferric form in the film is converted to the ferrous form on the forward scan and reconverted from ferrous to ferric form on the reverse scan. The similar CV peak currents for gold electrodes coated with a single layer or multilayers of enzyme suggest that only the first enzyme layer was electroactive, as also found for other hemoproteins in polyion films on smooth gold resonator electrodes [13,25].

The increase in the reduction signal and the disappearance of the oxidation signal observed by voltammetry (Fig. 3A) and amperometry (Fig. 3B) of the enzyme electrode in the presence of oxygen suggest coupling of the CYP3A4 redox reaction with the dioxygen binding to the reduced CYP3A4. The re-appearance of oxidation peak at scan rates higher than 500 mV/s suggests that the rate of binding of oxygen to the reduced CYP3A4 may be slower than this scan rates. Thus, the re-oxidation of reduced hemoprotein could be observed at high scan rates even in the presence of oxygen. As confirmed spectroscopically for reduction of myoglobin–dioxygen complexes [28], it is likely that the CYP3A4 (Fe^{II}) generated by electrochemical reduction reacts readily with dioxygen in the films as in nature, followed most likely by the electrochemical reduction of CYP3A4 (Fe^{II})O_2. Thus, this is a key reduction in the catalytic oxidation cycle of heme enzymes [29]. Direct reduction of oxygen on these electrodes occurs only at a more negative potential, about −500 mV [13]. Detection of significantly more H_2O_2 after electrolysis using the CYP3A4 film compared to electrolysis without CYP3A4 suggests a P450-mediated reduction of O_2 to H_2O_2, as auto-oxidation of the CYP3A4 (Fe^{II})O_2 complex with a rate constant of 2×10^{-6} s^{-1} is too slow to be important for catalytic production of H_2O_2 [30].

Under anaerobic conditions, addition of verapamil to the solution showed no change in the reduction potential of CYP3A4 in films. This is contrary to results reported by Kazlauskaite *et al*. [11] and Sligar and Gunsalus [31] for CYP101. They observed a positive shift on the reduction potential of CYP101 in the presence of its substrate. The most likely explanation would be that verapamil is not displacing water as the sixth axial ligand from the active site. Thus, no conversion of the heme to high spin would occur, and without spin shift the reduction potential is also unchanged. No spin shift has also been described for binding of other CYP3A4 substrates in different experimental settings [32]; thus, the absence of reduction potential shift does not imply a lack of substrate binding.

Under aerobic conditions in the presence of a substrate, voltammograms showed an increase in the catalytic reduction current for oxygen (Fig. 4). This reflects an increase in turnover of dioxygen affected by the substrate, and suggests that substrate is metabolized by CYP3A4, which is in turn regenerated for the next catalytic cycle. Changes in reduction currents measured in amperometric and voltammetric experiments upon the addition of substrates were dependent on substrate concentration, and represent biosensor transduction. The apparent K_m values obtained for the substrates tested were two orders of magnitude higher than the corresponding values published for microsomal incubations with MDZ [33], quinidine [34], and progesterone [35], and enzyme saturation was not observed at the highest substrate concentrations that could be dissolve in the buffer. Possible explanations for this phenomenon, include (i) rate-limiting diffusion of the substrate to the immobilized enzyme across the Helmholtz layer causing that the effective substrate concentration in the enzyme film was much lower than that in bulk; (ii) absence of a lipid bilayer as part of the active enzyme complex in CYP3A4 films compared to microsomal preparations, an effect which has previously been reported to decrease substrate affinity of purified enzyme in the presence of detergent [36,37]; or (iii) a change of enzyme affinity to the substrate caused by structural changes during the immobilization procedure. Further experiments are required to clarify this issue.

Product analyses after the electrolysis with the enzyme film confirmed the catalytic activity of the biosensor. The observed time-dependent product formation suggests that the activity of the enzyme remains constant throughout the electrolysis. Metabolites formed by electrode-driven enzyme catalysis are the same as produced by the microsomal incubation of human CYP3A4 with an NADPH generating system and corresponding substrates [38,39]. The product formation rates for electrochemically produced verapamil and MDZ metabolites are comparable to those found for the microsomal incubations when taking CYP3A4 content in a microsomal preparations into account. This rate is also comparable to the product formation rates achieved in electrochemically driven P450-catalyzed conversion of camphor [40] and progesterone [41].

The results obtained from the various electrolyses suggest that different mechanisms may involved in CYP3A4 electrode-driven metabolism of verapamil or MDZ. A minor role of reactive oxygen species in the formation of metabolites was identified. Whereas H_2O_2 was formed at the CYP3A4-coated electrode and made a small contribution to metabolite formation, there was no evidence for O_2^- to mediate verapamil or MDZ metabolism (Table 1). Thus, it appears that the major fraction of metabolites was formed by completion of the natural catalytic cycle of CYP3A4. Further studies will be required to understand all the reaction steps in this electrochemical-driven enzyme catalysis.

Despite this limitation, our results suggest that the human enzyme immobilized on the gold electrode is

electrically and catalytically active. Besides, using this kind of enzyme electrode, the natural electron delivery system which is necessary for the CYP catalytic cycle can be replaced by an electromotive force. In conclusion, our work has demonstrated the feasibility of utilizing adsorption of human CYP3A4 on top of a polycation layer on conventional gold electrodes for construction of a biosensor for P450s. Thus, important requirements for the application of human CYP biosensors in order to identify drugs or drug candidates as substrates or inhibitors to the attached enzyme are fulfilled.

Acknowledgments

We are grateful to Prof. Dr. M. Eichelbaum, O. Richter, and Dr. U. Hofmann (Dr. Margarete Fischer, Bosch, Institut für klinische Pharmakologie, Stuttgart, Germany) for analyzing concentrations of verapamil metabolites and to Dr. D. Lang for analyzing concentrations of MDZ metabolites (Bayer AG, Abt. Metabolismus und Isotopenchemie, Wuppertal, Germany).

References

[1] Ortiz de Montellano PR, Correia MA. Suicidal destruction of cytochrome P-450 during oxidative drug metabolism. Annu Rev Pharmacol Toxicol 1983;23:481–503.
[2] Tinel M, Belgiti J, Descatoire V, Amouyal G, Letteron P, Geneve J, Larrey D, Pessayre D. Inactivation of human liver cytochrome P-450 by the drug methoxsalen and other psoralen derivatives. Biochem Pharmacol 1987;36:951–5.
[3] Hedgaad J, Gunsalus IC. Mixed function oxidation. IV. An induced methylene hydroxylase in camphor oxidation. J Biol Chem 1965;240: 4038–43.
[4] Brøsen K. Recent developments in hepatic drug oxidation. Implications for clinical pharmacokinetics. Clin Pharmacokinet 1990;18: 220–39.
[5] Wang J. Amperometric biosensors for clinical and therapeutic drug monitoring. J Pharm Biomed Anal 1998;19:47–53.
[6] Hall EAH. Biosensoren. Heidelberg, Germany: Springer-Verlag; 1995.
[7] Armstrong FA, Herring HA, Hirst J. Reaction of complex metalloproteins studied by protein-film voltammetry. J Chem Soc Rev 1997; 26:169–79.
[8] Rusling JF. Enzyme bioelectrochemistry in cast biomembrane-like films. Acc Chem Res 1998;31:363–9.
[9] Hara M. Application of P450s for biosensing: combination of biotechnology and electrochemistry. Mater Sci Eng 2000;12:103–9.
[10] Iwuoha EI, Joseph S, Zhang Z, Smyth MR, Fuhr U, Oritz de Montellano PR. Drug metabolism biosensors: electrochemical reactivities of cytochrome P450cam immobilised in synthetic vesicular systems. J Pharm Biomed Anal 1998;17:1101–10.
[11] Kazlauskaite J, Westlake ACG, Wang LL, Hill HAO. Direct electrochemistry of cytochrome P-450cam. Chem Commun 1996;1:2189–90.
[12] Zhang Z, Nassar AF, Lu Z, Schenkman JB, Rusling JF. Direct electron injection from electrodes to cytochrome P-450cam in biomembrane-like films. J Chem Soc, Faraday Trans 1997;93:1769–74.
[13] Lvov YM, Lu Z, Schenkman JB, Zu X, Rusling JF. Direct electrochemistry of myoglobin and cytochrome P-450cam in alternate layer-by-layer films with DNA and other polyions. J Am Chem Soc 1998; 120:4073–80.
[14] Lei C, Wollenberger U, Jung C, Scheller FW. Clay-bridged electron transfer between cytochrome p450(cam) and electrode. Biochem Biophys Res Commun 2000;268:740–4.
[15] Sugihara N, Ogoma Y, Abe K, Kondo Y, Akaike T. Immobilization of cytochrome P-450 and electrochemical control of its activity. Polym Adv Technol 1998;9:307–13.
[16] Zu X, Lu Z, Zhang Z, Schenkman JB, Rusling JF. Electroenzyme-catalyzed oxidation of styrene and *cis*-methylstyrene using thin films of cytochrome P450cam and myoglobin. Langmuir 1999;15:7372–7.
[17] Hara M, Yasuda Y, Toyotama H, Ohkawa H, Nozawa T, Miyake J. A novel ISFET-type biosensor based on P450 monooxygenases. Biosens Bioelectron 2002;17:173–9.
[18] Shumyantseva VV, Bulko TV, Bachmann TT, Bilitewski U, Schmid RD, Archakov AI. Electrochemical reduction of flavocytochromes 2B4 and 1A2 and their catalytic activity. Arch Biochem Biophys 2000; 377:43–8.
[19] Pritchard MP, Ossetian R, Li DN, Henderson CJ, Burchell B, Wolf CR, Friedberg T. A general strategy for the expression of recombinant human cytochrome P450s in *Escherichia coli* using bacterial signal peptides: expression of CYP3A4, CYP2A6, and CYP2E1. Arch Biochem Biophys 1997;345:342–54.
[20] Sauerbrey GZ. Verwendung von Schwingquarzen zur Wägung dünner Schichten und zur Mikrowägung. Z Phys 1959;155:206–22.
[21] Lvov Y, Ariga K, Ichinose I, Kunitake T. Assembly of multicomponent protein by means of electrostatic layer-by-layer adsorption. J Am Chem Soc 1995;117:6117–23.
[22] Creighton TE. Protein structure, a practical approach. Oxford, New York, Tokyo: IRL Press; 1990. p. 43–55.
[23] Von Richter O, Eichelbaum M, Schonberger F, Hofmann U. Rapid and highly sensitive method for the determination of verapamil, [2H7]verapamil and metabolites in biological fluids by liquid chromatography-mass spectrometry. J Chromatogr B 2000;738:137–47.
[24] Shiro Y, Fujii M, Isogai Y, Adachi S, Iizuka T, Obayashi E, Makino R, Nakahara K, Shoun H. Iron-ligand structure and iron redox property of nitric oxide reductase cytochrome P450nor from *Fusarium oxysporum*: relevance to its NO reduction activity. Biochemistry 1995;34: 9052–8.
[25] Rusling JF. Electroactive and enzyme-active protein–polyion films assembled layer by layer. In: Mohwald H, Lvov YM, editors. Protein architecture: interfacing molecular assemblies and immobilization biotechnology. New York: Marcel Dekker; 2000. p. 337–54.
[26] Lvov YM. Electrostatic layer-by-layer assembly of proteins and polyions. In: Mohwald H, Lvov YM, editors. Protein architecture: interfacing molecular assemblies and immobilization biotechnology. New York: Marcel Dekker; 2000. p. 125–67.
[27] Murray RW. Chemically modified electrodes. In: Bard AJ, editor. Electroanalytical chemistry. New York: Marcel Dekker; 1984. p. 191–368.
[28] Onuoha C, Zu X, Rusling JF. Electrochemical generation and reactions of ferrylmyoglobins in water and microemulsions. J Am Chem Soc 1997;119:3979–86.
[29] Black SD, Coon MJ. P-450 cytochromes: structure and function. Adv Enzymol Relat Areas Mol Biol 1987;60:35–87.
[30] Wazawa T, Matsuoka A, Tajima G, Sugawara Y, Nakamura K, Shikama K. Hydrogen peroxide plays a key role in the oxidation reaction of myoglobin by molecular oxygen. A computer simulation. Biophys J 1992;63:544–50.
[31] Sligar SG, Gunsalus IC. A thermodynamic model of regulation: modulation of redox equilibria in camphor monoxygenase. Proc Natl Acad Sci USA 1976;73:1078–82.
[32] Yamazaki H, Johnson WW, Ueng YF, Shimada T, Guengerich FP. Lack of electron transfer from cytochrome b5 in stimulation of catalytic activities of cytochrome P450 3A4. Characterization of a reconstituted cytochrome P450 3A4/NADPH-cytochrome P450 re-

ductase system and studies with apo-cytochrome b5. J Biol Chem 1996;271:27438–44.
[33] Wang JS, Wen X, Backman JT, Taavitsainen P, Neuvonen PJ, Kivisto KT. Midazolam alpha-hydroxylation by human liver microsomes in vitro: inhibition by calcium channel blockers, itraconazole and ketoconazole. Pharmacol Toxicol 1999;85:157–61.
[34] Ngui JS, Tang W, Stearns RA, Shou M, Miller RR, Zhang Y, Lin JH, Baillie TA. Cytochrome P450 3A4-mediated interaction of diclofenac and quinidine. Drug Metab Dispos 2000;28:1043–50.
[35] Yamazaki H, Shimada T. Progesterone and testosterone hydroxylation by cytochromes P450 2C19, 2C9, and 3A4 in human liver microsomes. Arch Biochem Biophys 1997;346:161–9.
[36] Hara M, Miyake J, Asada Y, Ohkawa H. Purified fusion enzyme between rat cytochrome P4501A1 and yeast NADPH-cytochrome P450 oxidoreductase. Biosci Biotechnol Biochem 1999;63: 21–8.
[37] Brian WR, Sari MA, Iwasaki M, Shimada T, Kaminsky LS, Guengerich FP. Catalytic activities of human liver cytochrome P-450 IIIA4 expressed in *Saccharomyces cerevisiae*. Biochemistry 1990;29: 11280–92.
[38] Busse D, Cosme J, Beaune P, Kroemer HK, Eichelbaum M. Cytochromes of the P450 2C subfamily are the major enzymes involved in the *O*-demethylation of verapamil in humans. Naunyn Schmiedebergs Arch Pharmacol 1995;353:116–21.
[39] Ghosal A, Satoh H, Thomas PE, Bush E, Moore D. Inhibition and kinetics of cytochrome P4503A activity in microsomes from rat, human, and cDNA-expressed human cytochrome P450. Drug Metab Dispos 1996;24:940–7.
[40] Reipa V, Mayhew MP, Vilker VL. A direct electrode-driven P450 cycle for biocatalysis. Proc Natl Acad Sci USA 1997;94:13554–8.
[41] Estabrook RW, Faulkner KM, Shet MS, Fisher CW. Application of electrochemistry for P450-catalyzed reactions. Methods Enzymol 1996;272:44–51.